

1 **A biosynthetic platform for antimalarial drug discovery**

2 Mark D. Wilkinson¹, Hung-En Lai², Paul S. Freemont² and Jake Baum³

3 ¹Department of Chemistry, Imperial College London, UK

4 ²Department of Infectious Diseases, Faculty of Medicine, Imperial College London, UK

5 ³Department of Life Sciences, Imperial College London, UK

6

7 **Correspondence to:**

8 Jake Baum (jake.baum@imperial.ac.uk), Department of Life Sciences, Imperial College

9 London, Exhibition Road, South Kensington, London SW7 2AZ, United Kingdom

10 Paul Freemont (p.freemont@imperial.ac.uk), Department of Infectious Diseases, Imperial

11 College London, Exhibition Road, South Kensington, London SW7 2AZ, United Kingdom

12

13 **Running Title:** Biosynthesis of violacein as an antimalarial

14 **ABSTRACT**

15 Advances in synthetic biology have enabled production of a variety of compounds using
16 bacteria as a vehicle for complex compound biosynthesis. Violacein, a naturally occurring
17 indole pigment with antibiotic properties, can be biosynthetically engineered in *Escherichia*
18 *coli* expressing its non-native synthesis pathway. To explore whether this synthetic
19 biosynthesis platform could be used for drug discovery, here we have screened bacterially-
20 derived violacein against the main causative agent of human malaria, *Plasmodium falciparum*.
21 We show the antiparasitic activity of bacterially-derived violacein against the *P. falciparum*
22 3D7 laboratory reference strain as well as drug-sensitive and resistant patient isolates,
23 confirming the potential utility of this drug as an antimalarial. We then screen a biosynthetic
24 series of violacein derivatives against *P. falciparum* growth. The demonstrated varied activity
25 of each derivative against asexual parasite growth points to potential for further development
26 of violacein as an antimalarial. Towards defining its mode of action, we show that biosynthetic
27 violacein affects the parasite actin cytoskeleton, resulting in an accumulation of actin signal
28 that is independent of actin polymerization. This activity points to a target that modulates
29 actin behaviour in the cell either in terms of its regulation or its folding. More broadly, our
30 data show that bacterial synthetic biosynthesis could become a suitable platform for
31 antimalarial drug discovery with potential applications in future high-throughput drug
32 screening with otherwise chemically-intractable natural products.

33

34 **KEYWORDS**

35 Violacein; drug discovery; synthetic biology; antimalarial

36

37 INTRODUCTION

38 Malaria has a huge global health burden, with around half of the world's population at risk of
39 contracting the disease which killed over 400 000 people in 2017(1). Malaria disease is caused
40 by apicomplexan parasites from the genus *Plasmodium*, with *Plasmodium falciparum* causing
41 the majority of deaths worldwide. The symptoms of malaria disease develop during the
42 asexual stages of the parasite life cycle, which occurs in the blood stream. Here, the parasite
43 undergoes multiple rounds of growth, replication and invasion of red blood cells. Various
44 drugs have been developed to target the asexual stages of the parasite but, inevitably,
45 resistance has evolved to every major front-line therapy for malaria treatment including,
46 most recently, artemisinin combined therapies (ACTs)(2). Multi-drug resistance to ACTs,
47 focussed in the Greater Mekong Subregion of South East Asia, has been reported both as
48 delayed parasite clearance and, more worryingly, treatment failure(3). The challenges of
49 emerging drug resistance combined with the cost associated with development of new drugs
50 make it essential to explore new ways to develop novel antimalarial compounds.

51

52 Previous work identified violacein, a violet indolocarbazole pigment produced by bacteria
53 (Fig. 1a), as a potential antimalarial able to kill both asexual *P. falciparum* parasites *in vitro*
54 and protect against malaria infection in a mouse malaria model *in vivo*(4–6). Violacein's
55 antimalarial activity has therefore identified it as a potential for future drug development.
56 However, commercial violacein samples can only be obtained through laborious purification
57 from bacteria (*Chromobacterium*(7, 8) or *Janthinobacterium*(9)) because of the complexity of
58 its highly aromatic structure (Fig. 1a). Purification from these bacteria requires specialised
59 equipment and high-level biosafety equipment since these bacteria themselves can cause
60 deadly infections(10). As such, commercially available violacein is extremely expensive.

61 Alternative strategies of violacein synthesis are being explored, in particular the use of
62 synthetic biology to engineer industrial bacterial species that can express non-native
63 violacein. Several groups including ours(11) have been successful in implementing a five-gene
64 violacein biosynthetic pathway (vioABCDE) into *Escherichia coli* or other heterologous
65 hosts(12–14), providing a route for robust, in-house and inexpensive compound production.

66

67 We have previously extended the success of this biosynthetic pathway by generating
68 combinations of 68 new violacein and deoxyviolacein analogues. These combinations are
69 achieved by feeding various tryptophan substrates to recombinant *E. coli* expressing the
70 violacein biosynthetic pathway or via introduction of an *in vivo* chlorination step - the
71 tryptophan 7-halogenase RebH from the rebeccamycin biosynthetic pathway(13, 15–17). This
72 biosynthetic approach is able to produce large quantities of compound derivatives using
73 simple, cheap and non-hazardous bacteria compared to native producing strains in a
74 sustainable and flexible approach.

75

76 Here, we set out to explore whether use of this biosynthetic system could be developed as a
77 route to antimalarial compound production and testing, measuring the activity of derivatives
78 on the growth of *P. falciparum* sexual and asexual parasites. We have confirmed the viability
79 of the system, ensuring there is no background antiparasitic activity in bacterial solvent
80 extracts lacking violacein. We then tested the biosynthetic violacein extract from *E. coli* and
81 confirmed its half maximal inhibitory concentration (IC50) in agreement with a commercial
82 violacein standard and previous studies(14). Finally, as well as using this approach to explore
83 the mode of action of violacein, we show that extracts representing a diverse series of
84 biosynthetically derived variants show varying effects on parasite growth, with 16 of the 28

85 compound mixtures inhibiting growth to a greater level than the parent violacein molecule.
86 Indeed, one purified compound, 7-chloroviolaicin, exhibits a ~20% higher inhibition activity
87 than the underivatized violacein compound. The screening approach used in this study
88 suggests that biosynthetic systems may therefore provide an, as yet, untapped resource for
89 screening complex compounds and optimising them for antimalarial discovery.

90

91 RESULTS

92 **Violacein expressed using synthetic operons kills *P. falciparum* 3D7 parasites**

93 Previous work has shown that violacein is able to kill asexual *Plasmodium* parasites *in vitro*
94 and in a mouse model *in vivo*(9, 13). Violacein cytotoxicity is highly dependent on cell type,
95 ranging from an IC50 value of around 2.5 μ M in HepG2 cells to up to 12 μ M in fibroblasts and
96 potential erythrocytic rupture at concentrations above 10 μ M(18, 19). Taking this into
97 consideration, we used concentrations of 2 μ M violacein or less to explore growth inhibition
98 of *P. falciparum* asexual stages, noting no phenotypic effect on erythrocyte morphology at
99 the highest final concentration (Fig. S1). Our biosynthetic system for violacein production
100 requires chloramphenicol drug pressure, which is known to affect parasite viability(20). We
101 first set out to ensure presence of this known antibiotic did not affect parasite growth. Extract
102 from bacteria lacking the violacein producing enzymes but grown under chloramphenicol
103 pressure (i.e. background) did not affect parasite viability (Fig. S2). This gave us confidence
104 that extracts from biosynthetically modified *E. coli* would report only on the activity of a drug
105 produced but not from background chloramphenicol contamination. To test this, we
106 compared the activity of a commercial violacein standard (Vio-Sigma) with violacein derived
107 from bacterial solvent extracts from *E. coli* biosynthesis (Vio-Biosyn) on wild-type 3D7 *P.*
108 *falciparum* growth, using a well-established asexual growth inhibition assay. No difference in
109 the IC50 values between the two violacein samples was seen (Figs. 1b-c). We further tested
110 the two violacein samples on sexual parasites by measuring exflagellation(21) and saw no
111 difference in the IC50 values of around 1.7 μ M (Fig. S3) but complete IC50 curves could not
112 be generated without going above the cytotoxic threshold of 2.5 μ M. All these data
113 demonstrate that solvent extracted violacein from *E. coli*, Vio-Biosyn, is active and that its

114 production provides a suitable platform for development and testing of potential antimalarial
115 compounds.

116

117 **Biosynthetic violacein extract kills both artemisinin-resistant and -sensitive field isolate** 118 **parasites**

119 To explore whether violacein has utility for addressing emerging ACT drug resistance in the
120 field, we tested the efficacy of Vio-Sigma and Vio-Biosyn on two parasite clinical isolates
121 deriving from the Greater Mekong subregion, where ACT resistance is concentrated. Both
122 clinical isolates have been phenotypically characterised in clinic, showing either treatment
123 failure or success, adapted to culture and genotyped for the C580Y Kelch-13 resistance
124 marker(22) known to correlate with sensitivity to artemisinin-based drugs. Both the
125 artemisinin-sensitive isolate (ANL1, Kelch13 wild-type) and the artemisinin-resistant isolate
126 (APL5G, Kelch13 C580Y) were sensitive to Vio-Biosyn and Vio-Sigma with similar IC50 values
127 (Figs. 2a-d). Activity against artemisinin-resistance provides support for development of the
128 violacein scaffold for addressing emerging drug-resistance in the field.

129

130 **Violacein derivatives show potent anti-malarial activity**

131 To explore whether bacterial biosynthesis could be utilised further to generate compound
132 derivatives, increasing the throughput of complex molecule testing, we obtained extracts
133 from 28 bacteria strains each modulated to synthesise a mixture of violacein analogues (Fig.
134 S4)(23). The bacterial extracts were produced by feeding corresponding tryptophan
135 substrates as described previously(14) and violacein concentrations in the extracts were
136 calibrated against a violacein standard. Asexual growth assays were again carried out, testing
137 each extract at the IC50 of biosynthetic violacein, 0.50 μ M. We saw a large variation of

138 inhibition of parasite growth, with 8 compound mixtures exhibiting >95% inhibition, whilst 12
139 others showed a decreased effect on parasite growth (Fig. 3a). As a proof-of-concept, one of
140 the more active extracts was used to purify the violacein derivative, 7-chloroviolaecin (Fig.
141 3b). 7-chloroviolaecin exhibited an IC50 value of 0.42 μ M. This purified derivative is at least
142 equipotent to the parent violacein compound (Fig. 3c). Given the speed and low cost of
143 extracting these violacein analogues and purifying them directly from bacteria, these data
144 therefore suggest an entirely new approach to complex compound drug-testing for
145 antimalarial discovery and optimisation.

146

147 **Biosynthetic violacein affects actin dynamics in the cell but does not affect polymerisation**

148 *in vitro*

149 The mode of action of violacein against *P. falciparum* parasites has not previously been
150 characterised. Treatment of a variety of human derived cell lines with violacein show a range
151 of responses, with one patient-derived glioblastoma cell line having compromised motility
152 and increased rounding up, attributed to a disruption of the filamentous actin network(24).
153 Towards exploring the phenotype associated with its activity we performed flow cytometry
154 and immunofluorescence assays (IFAs) to observe any changes in the parasite under
155 biosynthetic violacein treatment. A 3D7-derived parasite line expressing a constitutive
156 cytoplasmic green fluorescent protein (sfGFP) marker was labelled with DNA marker DAPI
157 (4',6-diamidino-2-phenylindole) and a monoclonal antibody that preferentially recognises
158 filamentous actin(25, 26) to explore overall parasite morphology: cytoplasm, nucleus and
159 actin cytoskeleton respectively. Parasites were then treated with either negative, dimethyl
160 sulfoxide (DMSO), or positive, actin filament stabilising compound, jasplakinolide (JAS)
161 controls as well as Vio-Biosyn. Parasites were checked by flow cytometry for any differences

162 in overall signal (Fig. S5). A low actin-positive signal was seen with DMSO treatment, as
163 expected given the predominance of short, transient filaments and globular actin in asexual
164 parasites(27). The intensity of actin labelling following JAS and violacein treatment both,
165 however, showed marked increases when compared to DMSO (Fig. S5).

166

167 To explore the nature of flow-cytometry changes in actin intensity following violacein
168 treatment, IFAs were undertaken. In the DMSO-treated parasites, the GFP signal is spread
169 throughout the cytoplasm along with a clearly defined nucleus as expected (Fig. 4a). The actin
170 signal is diffuse with a low background (Fig. 4a). Following JAS treatment, actin filaments are
171 known to be stabilised(27) producing an expected concentrated overall actin signal (Fig. 4b),
172 indicative of high local concentrations of polymerized actin. Parasites treated with Vio-Biosyn
173 also gave a much higher actin signal than untreated controls, though distinct from that
174 following JAS treatment (Fig. 4c). The concentrated signal from Vio-Biosyn was broader across
175 the cell and less focussed in localised regions of the cell periphery. This matched the overall
176 intensity of signal seen by flow-cytometry and relative to sfGFP signal as a control for parasite
177 size (Fig. 4d). In the DMSO-treated control, the diffuse actin signal is 3% of total GFP signal.
178 This increases to 27% upon JAS treatment, indicative of an increased number of filaments,
179 whereas parasites treated with Vio-Biosyn reach a mean average signal 98%, representing a
180 huge increase in actin accumulation in the cell. This broad concentration of actin signal would
181 be indicative of either massively increased filament nucleation or actin aggregation as caused
182 by actin misfolding. To test whether Vio-Biosyn directly affects actin filament formation (as
183 JAS does), both drugs were assayed using a pyrene-labelled actin assembly assay, used
184 previously to test compound derivatives for actin activity(27). No effect on actin
185 polymerisation was seen with Vio-Biosyn when compared to either JAS (filament nucleating)

186 or the monomer-stabilising drug latrunculin B (Fig. 4d). Together, these observations suggest
187 Vio-Biosyn does not directly interact with actin. It is therefore possible that Vio-Biosyn
188 interacts with actin indirectly such as via the known actin-binding partners in the parasite
189 cell(28) or via an alternative pathway involved in actin folding, which would give rise to actin
190 aggregation within the cell.

191

192

193 **DISCUSSION**

194 The emergence of resistance to front-line artemisinin-based drug treatments for malaria is a
195 major threat to global health. As such, new antimalarial treatments are in urgent demand.
196 Here, we tested violacein, a compound with known antibacterial, antitumorigenic and
197 antiparasitic activity, against *P. falciparum* parasites validating its potential utility for
198 antimalarial drug development. We showed that biosynthetically produced violacein was as
199 effective as commercially available violacein, with a mode of action that affects the actin
200 cytoskeleton of the parasite. We also tested 28 violacein analogue mixtures using a high-
201 throughput growth assay on asexual parasites suggesting this method of biosynthetic
202 production is a suitable platform for antimalarial discovery and optimisation.

203

204 Previous work has shown that violacein is capable of killing lab-derived chloroquine-resistant
205 *P. falciparum* parasites(14). Here, we showed that patient-sourced clinical isolates, sensitive
206 or resistant to artemisinin, could equally be killed by both commercial and biosynthetic
207 violacein with similar IC50 values. Our results show violacein inhibits asexual parasite growth
208 with an IC50 value of at least an order of magnitude more potent than fibroblasts and
209 lymphocytes found in circulation in the blood (0.5 μ M vs > 10 μ M)(18, 19). Furthermore,

210 although full IC50 curves could not be generated, the compounds both inhibit development
211 of the sexual stages of the parasite life cycle with an IC50 of around 1.7 μM (Fig. S3). Any
212 compound identified using this assay with an IC50 of less than 2.0 μM is considered for further
213 compound development(29). Combined, these data suggest violacein is a potential drug that
214 could be developed to antagonize resistance in the field and target both asexual and sexual
215 stage parasites. Whilst the derivative library tested consisted of mixtures of violacein
216 analogues, it is encouraging to see some of these compound mixtures have considerably more
217 potent anti-malarial activity than violacein itself. Critically, when we tested a purified
218 compound (7-chloroviolaicin) we saw at least equipotent activity of the derivative
219 compound, illustrating the potential of biosynthetic production of antimalarial compounds
220 for rapid screening and rational drug optimisation.

221

222 Interestingly, violacein-treated parasites have cytoskeletal deformities that suggested
223 disruption to actin modulation within the parasite. Given violacein has no effect on actin
224 polymerisation kinetics *in vitro*, it is possible that the phenotype observed is as a result actin
225 aggregation in the cell, which could be a side effect of actin misfolding. *P. falciparum* requires
226 actin as an essential part of its motor complex and for other processes in the cell(9). Unlike
227 most proteins, actin requires a dedicated chaperonin system to fold into its native state(30).
228 Of note, this entire pathway is highly upregulated in artemisinin-resistant parasite isolates(31)
229 and would constitute a well-justified target for antagonising drug resistance in the field.
230 Further work in testing the effects of violacein on actin folding or modulation are clearly
231 required to explore whether this is the target for the drug. Ultimately, the ability of violacein
232 to affect such a major pathway as actin dynamics in the cell, as well as kill drug-resistant
233 parasites, provides an encouraging outlook for its therapeutic development.

234

235 In summary, our data show that a bacterial biosynthetic platform for creating compounds and
236 their derivatives is suitable for testing for antimalarial drug development. As the need for
237 novel therapeutics increases and interest in natural compounds, often complex in nature,
238 grows we hope to use this approach to develop novel chemical scaffolds in a high throughput
239 manner towards finding the next generation of antimalarials.

240

241 **METHODS**

242 **Generation and extraction of violacein and derivatives**

243 Violacein and derivatives were generated and extracted as previously described(32). Briefly,
244 *E. coli* JM109 strain (Promega) was transformed with the violacein pathway plasmid
245 (pTU2S(VioAE)-b-VioBCD) and grown overnight before being inoculated into LB broth until
246 OD600 reaches 0.5. These cultures were then supplemented with either tryptophan or a
247 synthetic tryptophan analogue at 0.04% (w/v) and grown at 25 °C for up to 65 h before
248 pelleted at 4000 rpm. The cell pellet was then resuspended with 1/10th volume of ethanol to
249 extract violacein, followed by centrifugation to separate ethanol supernatant containing
250 violacein extract from cell debris. The supernatant was then dried *in vacuo* and stored at -20
251 °C for long-term storage or reconstituted in DMSO for growth inhibition assays.
252 Concentrations of violacein in the bacterial solvent extracts were calibrated against
253 commercial violacein standard (Sigma) based on absorbance at 575 nm. Compound mixtures
254 used in the growth inhibition assay consist of mixtures of violacein derivatives (Fig. S4) as
255 described previously(14).

256

257 ***Plasmodium falciparum* growth inhibition assays**

258 *P. falciparum* parasite lines 3D7, ANL1, APL5G were used for the GIAs. A 3D7 sfGFP line was
259 used for immunofluorescence assays(33). All parasite lines were cultured in complete RPMI
260 (RPMI-HEPES culture media (Sigma) supplemented with 0.05 g/L hypoxanthine, 0.025 g/L
261 gentamicin and 5 g/L Albumax II (ThermoScientific) and maintained at 1% to 5% parasitaemia
262 and 4% haematocrit. For the growth inhibition assay (GIA), 96-well plates were pre-dispensed
263 with a serial dilution of compound and normalised to 1% DMSO. Double-synchronised ring-
264 stage parasites (1% parasitaemia, 2% haematocrit, complete media, sorbitol synchronised at
265 ring stage at 0 hrs and 48 hrs) were added to the wells to a total volume of 101 μ L. Cultures
266 were incubated for 72 h at 37 °C in a gas mixture of 90% N₂, 5% O₂, 5% CO₂. Red blood cells
267 were lysed through freeze-thaw at -20 °C and parasites were resuspended and lysed with 100
268 μ L lysis buffer (20 mM TRIS-HCL pH 7.5, 5 mM EDTA, 0.008% saponin, 0.8% Triton-X 100)
269 containing 0.2% SYBR green and incubated for 1 h at room temperature. SYBR green
270 fluorescence (excitation 485 nm / emission 535 nm) was measured using a Tecan infinite
271 M200 Pro. Data shown is the mean average of 3 biological replicates (\pm SEM), each of which
272 is a mean average of 3 technical replicates (unless stated otherwise), and is normalised to a
273 positive control (cycloheximide) and a negative control (DMSO only). IC₅₀ values were
274 calculated using GraphPad Prism version 8.0.

275

276 **Immunofluorescence assays**

277 100 μ L of mixed stage sfGFP parasite line (5% parasitaemia, 2% haematocrit) was incubated
278 for 24 h with 2 μ M of the compound of interest. At t=0 h and t=6 h, parasites were fixed with
279 4% paraformaldehyde, 2% glutaraldehyde (Electron Microscopy Sciences) and incubated on
280 a roller for 20 mins at room temperature (RT), before being pelleted at 3000 RPM and washed
281 three times in 100 μ L 1 X phosphate-buffered saline (PBS). The cells were subsequently

282 permeabilised in 0.1% Triton-X 100 (Sigma) for 10 mins at RT before being pelleted and
283 washed three times in PBS as before. Cells were blocked in 3% bovine serum albumin (BSA)
284 in PBS for 1 h at RT on a roller before being incubated with primary antibody (1:500 mouse
285 anti-actin 5H3(14)) for 1 h at RT. Cells were washed three times with PBS before addition of
286 the secondary antibody (1:1000 anti-mouse Alexa 647 conjugated) for 1 h at RT. Cells were
287 washed three times in PBS and resuspended in 100 μ L PBS with 0.05% DAPI. Cells were diluted
288 30-fold and loaded onto polylysine-coated coverslips (ibidi) before being imaged. Imaging was
289 performed on a Nikon Ti-E microscope using a 100 x Plan Apo 1.4 NA oil objective lens with
290 'DAPI', 'FITC' and 'Cy5' specific filtersets. Image stacks were captured 3 μ m either side of the
291 focal plane with a z-step of 0.2 μ m. Image analysis was conducted on raw image data sets in
292 ImageJ, calculating a ratio between AlexaFluor 647 and FITC by measuring the mean signal
293 intensity in a defined area of 88 nm². 62 images were captured for each sample from two
294 wells from two biological repeats. Images shown in Fig. 4 were deconvolved in Icy using the
295 EpiDemic Plugin and a maximum intensity projection was made in ImageJ.

296

297

298 **List of abbreviations**

299 DAPI – 4',6-diamidino-2-phenylindole

300 IFA – immunofluorescence assay

301 GIA – growth inhibition assay

302 JAS – Jasplakinolide

303 LatB – Latrunculin B

304

305 **REFERENCES**

306 1. 2019. WHO | World malaria report 2018. WHO.

307 2. Saunders DL, Vanachayangkul P, Lon C. 2014. Dihydroartemisinin–Piperaquine Failure
308 in Cambodia. *N Engl J Med* 371:484–485.

309 3. Kanoi BN, Takashima E, Morita M, White MT, Palacpac NMQ, Ntege EH, Balikagala B,
310 Yeka A, Egwang TG, Horii T, Tsuboi T. 2017. Antibody profiles to wheat germ cell-free
311 system synthesized Plasmodium falciparum proteins correlate with protection from
312 symptomatic malaria in Uganda. *Vaccine*.

313 4. Shaw PJ, Chaotheing S, Kaewprommal P, Piriyaopongsa J, Wongsombat C, Suwannakitti
314 N, Koonyosying P, Uthaipibull C, Yuthavong Y, Kamchonwongpaisan S. 2015.
315 Plasmodium parasites mount an arrest response to dihydroartemisinin, as revealed
316 by whole transcriptome shotgun sequencing (RNA-seq) and microarray study. *BMC*
317 *Genomics* 16:830.

318 5. Paloque L, Ramadani AP, Mercereau-Puijalon O, Augereau J-M, Benoit-Vical F. 2016.
319 Plasmodium falciparum: multifaceted resistance to artemisinins. *Malar J* 15:149.

320 6. Mbengue A, Bhattacharjee S, Pandharkar T, Liu H, Estiu G, Stahelin R V., Rizk SS,
321 Njimoh DL, Ryan Y, Chotivanich K, Nguon C, Ghorbal M, Lopez-Rubio J-J, Pfrender M,

- 322 Emrich S, Mohandas N, Dondorp AM, Wiest O, Haldar K. 2015. A molecular
323 mechanism of artemisinin resistance in Plasmodium falciparum malaria. Nature
324 520:683–687.
- 325 7. McLaughlin EC, Norman MW, Ko Ko T, Stolt I. 2014. Three-component synthesis of
326 disubstituted 2H-pyrrol-2-ones: preparation of the violacein scaffold. Tetrahedron
327 Lett 55:2609–2611.
- 328 8. Petersen MT, Nielsen TE. 2013. Tandem Ring-Closing Metathesis/Isomerization
329 Reactions for the Total Synthesis of Violacein. Org Lett 15:1986–1989.
- 330 9. Lopes SCP, Blanco YC, Justo GZ, Nogueira PA, Rodrigues FLS, Goelnitz U, Wunderlich
331 G, Facchini G, Brocchi M, Duran N, Costa FTM. 2009. Violacein Extracted from
332 Chromobacterium violaceum Inhibits Plasmodium Growth In Vitro and In Vivo.
333 Antimicrob Agents Chemother 53:2149–2152.
- 334 10. Pantanella F, Berlutti F, Passariello C, Sarli S, Morea C, Schippa S. 2006. Violacein and
335 biofilm production in Janthinobacterium lividum. J Appl Microbiol
336 0:061120055200056-???
- 337 11. Sneath PHA, Singh RB, Whelan JPF, Edwards D. 1953. Fatal infection by
338 Chromobacterium Violaceum. Lancet 262:276–277.
- 339 12. Rodrigues AL, Trachtmann N, Becker J, Lohanatha AF, Blotenberg J, Bolten CJ, Korneli
340 C, de Souza Lima AO, Porto LM, Sprenger GA, Wittmann C. 2013. Systems metabolic
341 engineering of Escherichia coli for production of the antitumor drugs violacein and
342 deoxyviolacein. Metab Eng 20:29–41.
- 343 13. Bilsland E, Tavella TA, Krogh R, Stokes JE, Roberts A, Ajioka J, Spring DR, Andricopulo
344 AD, Costa FTM, Oliver SG. 2018. Antiplasmodial and trypanocidal activity of violacein
345 and deoxyviolacein produced from synthetic operons. BMC Biotechnol 18:22.

- 346 14. Lai H-E, Obled AM, Chee SM, Morgan RM, Sharma S V, Moore SJ, Polizzi KM, Goss RJ,
347 Freemont PS. 2019. A GenoChemetic strategy for derivatization of the violacein
348 natural product scaffold. bioRxiv 202523.
- 349 15. Rodrigues AL, Göcke Y, Bolten C, Brock NL, Dickschat JS, Wittmann C. 2012. Microbial
350 production of the drugs violacein and deoxyviolacein: analytical development and
351 strain comparison. *Biotechnol Lett* 34:717–720.
- 352 16. Wang H, Jiang P, Lu Y, Ruan Z, Jiang R, Xing X-H, Lou K, Wei D. 2009. Optimization of
353 culture conditions for violacein production by a new strain of *Duganella* sp. B2.
354 *Biochem Eng J* 44:119–124.
- 355 17. Choi SY, Kim S, Lyuck S, Kim SB, Mitchell RJ. 2015. High-level production of violacein
356 by the newly isolated *Duganella violaceinigra* str. NI28 and its impact on
357 *Staphylococcus aureus*. *Sci Rep* 5:15598.
- 358 18. Bilsland E, Tavella TA, Krogh R, Stokes JE, Roberts A, Ajioka J, Spring DR, Andricopulo
359 AD, Costa FTM, Oliver SG. 2018. Antiplasmodial and trypanocidal activity of violacein
360 and deoxyviolacein produced from synthetic operons. *BMC Biotechnol* 18:22.
- 361 19. Leal AM de S, de Queiroz JDF, de Medeiros SRB, Lima TK de S, Agnez-Lima LF. 2015.
362 Violacein induces cell death by triggering mitochondrial membrane hyperpolarization
363 in vitro. *BMC Microbiol* 15:115.
- 364 20. Yeo AE, Rieckmann KH. 1994. The in vitro antimalarial activity of chloramphenicol
365 against *Plasmodium falciparum*. *Acta Trop* 56:51–4.
- 366 21. Ruecker A, Mathias DK, Straschil U, Churcher TS, Dinglasan RR, Leroy D, Sinden RE,
367 Delves MJ. 2014. A Male and Female Gametocyte Functional Viability Assay To
368 Identify Biologically Relevant Malaria Transmission-Blocking Drugs. *Antimicrob Agents*
369 *Chemother* 58:7292–7302.

- 370 22. Malpartida-Cardenas K, Miscourides N, Rodriguez-Manzano J, Yu L-S, Moser N, Baum
371 J, Georgiou P. 2019. Quantitative and rapid *Plasmodium falciparum* malaria diagnosis
372 and artemisinin-resistance detection using a CMOS Lab-on-Chip platform. *Biosens*
373 *Bioelectron* 145:111678.
- 374 23. Baum J, Papenfuss AT, Baum B, Speed TP, Cowman AF. 2006. Regulation of
375 apicomplexan actin-based motility. *Nat Rev Microbiol* 4:621–8.
- 376 24. Mehta T, Vercruyse K, Johnson T, Ejiofor AO, Myles E, Quick QA. 2015. Violacein
377 induces p44/42 mitogen-activated protein kinase-mediated solid tumor cell death
378 and inhibits tumor cell migration. *Mol Med Rep* 12:1443–1448.
- 379 25. Mbengue A, Bhattacharjee S, Pandharkar T, Liu H, Estiu G, Stahelin R V., Rizk SS,
380 Njimoh DL, Ryan Y, Chotivanich K, Nguon C, Ghorbal M, Lopez-Rubio J-J, Pfrender M,
381 Emrich S, Mohandas N, Dondorp AM, Wiest O, Haldar K. 2015. A molecular
382 mechanism of artemisinin resistance in *Plasmodium falciparum* malaria. *Nature*
383 520:683–687.
- 384 26. Miotto O, Amato R, Ashley EA, MacInnis B, Almagro-Garcia J, Amaratunga C, Lim P,
385 Mead D, Oyola SO, Dhorda M, Imwong M, Woodrow C, Manske M, Stalker J, Drury E,
386 Campino S, Amenga-Etego L, Thanh T-NN, Tran HT, Ringwald P, Bethell D, Nosten F,
387 Phyo AP, Pukrittayakamee S, Chotivanich K, Chuor CM, Nguon C, Suon S, Sreng S,
388 Newton PN, Mayxay M, Khanthavong M, Hongvanthong B, Htut Y, Han KT, Kyaw MP,
389 Faiz MA, Fanello CI, Onyamboko M, Mokuolu OA, Jacob CG, Takala-Harrison S, Plowe
390 C V, Day NP, Dondorp AM, Spencer CCA, McVean G, Fairhurst RM, White NJ,
391 Kwiatkowski DP. 2015. Genetic architecture of artemisinin-resistant *Plasmodium*
392 *falciparum*. *Nat Genet* 47:226–234.
- 393 27. Angrisano F, Riglar DT, Sturm A, Volz JC, Delves MJ, Zuccala ES, Turnbull L, Dekiwadia

394 C, Olshina MA, Marapana DS, Wong W, Mollard V, Bradin CH, Tonkin CJ, Gunning PW,
395 Ralph SA, Whitchurch CB, Sinden RE, Cowman AF, McFadden GI, Baum J. 2012. Spatial
396 Localisation of Actin Filaments across Developmental Stages of the Malaria Parasite.
397 PLoS One 7:e32188.

398 28. Johnson S, Rahmani R, Drew DR, Williams MJ, Wilkinson M, Tan YH, Huang JX, Tonkin
399 CJ, Beeson JG, Baum J, Smith BJ, Baell JB. 2016. Truncated Latrunculins as Actin
400 Inhibitors Targeting Plasmodium falciparum Motility and Host Cell Invasion. J Med
401 Chem 59.

402 29. Miguel-Blanco C, Molina I, Bardera AI, Díaz B, de las Heras L, Lozano S, González C,
403 Rodrigues J, Delves MJ, Ruecker A, Colmenarejo G, Viera S, Martínez-Martínez MS,
404 Fernández E, Baum J, Sinden RE, Herreros E. 2017. Hundreds of dual-stage
405 antimalarial molecules discovered by a functional gametocyte screen. Nat Commun
406 8:15160.

407 30. Das S, Lemgruber L, Tay CL, Baum J, Meissner M. 2017. Multiple essential functions of
408 Plasmodium falciparum actin-1 during malaria blood-stage development. BMC Biol
409 15:70.

410 31. Olshina MA, Baumann H, Willison KR, Baum J. 2015. Plasmodium actin is incompletely
411 folded by heterologous protein-folding machinery and likely requires the native
412 Plasmodium chaperonin complex to enter a mature functional state. FASEB J.

413 32. Mok S, Ashley EA, Ferreira PE, Zhu L, Lin Z, Yeo T, Chotivanich K, Imwong M,
414 Pukrittayakamee S, Dhorda M, Nguon C, Lim P, Amaratunga C, Suon S, Hien TT, Htut
415 Y, Faiz MA, Onyamboko MA, Mayxay M, Newton PN, Tripura R, Woodrow CJ, Miotto
416 O, Kwiatkowski DP, Nosten F, Day NPJ, Preiser PR, White NJ, Dondorp AM, Fairhurst
417 RM, Bozdech Z. 2015. Drug resistance. Population transcriptomics of human malaria

418 parasites reveals the mechanism of artemisinin resistance. *Science* 347:431–5.

419 33. Ashdown GW, Dimon M, Fan M, Terán FS-R, Witmer K, Gaboriau DCA, Armstrong Z,
420 Hazard J, Ando DM, Baum J. 2019. A machine learning approach to define antimalarial
421 drug action from heterogeneous cell-based screens. *bioRxiv* 2019.12.19.882480.

422

423

424 **DECLARATIONS**

425 **Acknowledgements**

426 Clinical isolates were provided by Professor Kesinee Chotivanich and Dr Huy Rekol (Director
427 of the National Centre for Parasitology, Entomology and Malaria Control) through a joint
428 Medical Research Council (MRC) and National Science Technology Development Agency
429 (NSTDA) award (MR/N012275/1 to JB), acknowledging support from the TRAC clinical studies,
430 funded through the UK Government Department for International Development (DFID). The
431 3D7 sfGFP line was provided by Dr Kathrin Witmer (Imperial College London). We wish to
432 acknowledge Thomas Blake for his help conducting the flow cytometry and Alisje Churchyard
433 for conducting the exflagellation inhibition assay.

434

435 **Funding**

436 MDW is funded by the EPSRC through the Institute of Chemical Biology at Imperial College
437 London. HEL is supported by an Imperial College President's PhD scholarship. This work was
438 supported by the EPSRC (EP/L011573/1 to PSF), the Wellcome Trust (100993/Z/13/Z to JB)
439 and the Human Frontier Science Programme (RGY0066/2016 to JB).

440

441 **Availability of data and materials**

442 The datasets used during the study are available from the corresponding author(s) upon
443 reasonable request.

444

445 **Author contributions**

446 MDW planned and performed the experiments and wrote the manuscript under the guidance
447 of JB. HEL created the violacein constructs and extracted violacein and its derivatives under
448 the guidance of PSF. All authors read, edited and approved the final manuscript.

449

450 **Ethics approval and consent to participate**

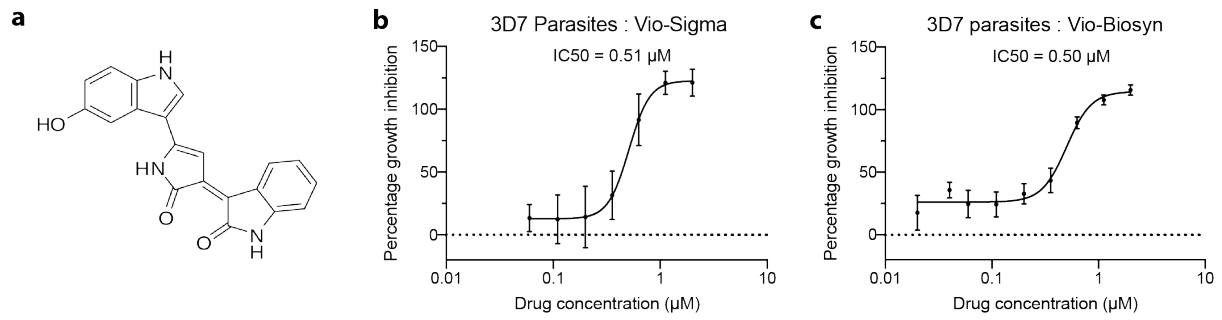
451 Not applicable.

452

453 **Competing interests**

454 The authors declare that they have no competing interests.

455 **FIGURES**



456

457 **Fig. 1:** *Plasmodium falciparum* asexual growth inhibition assays with violacein

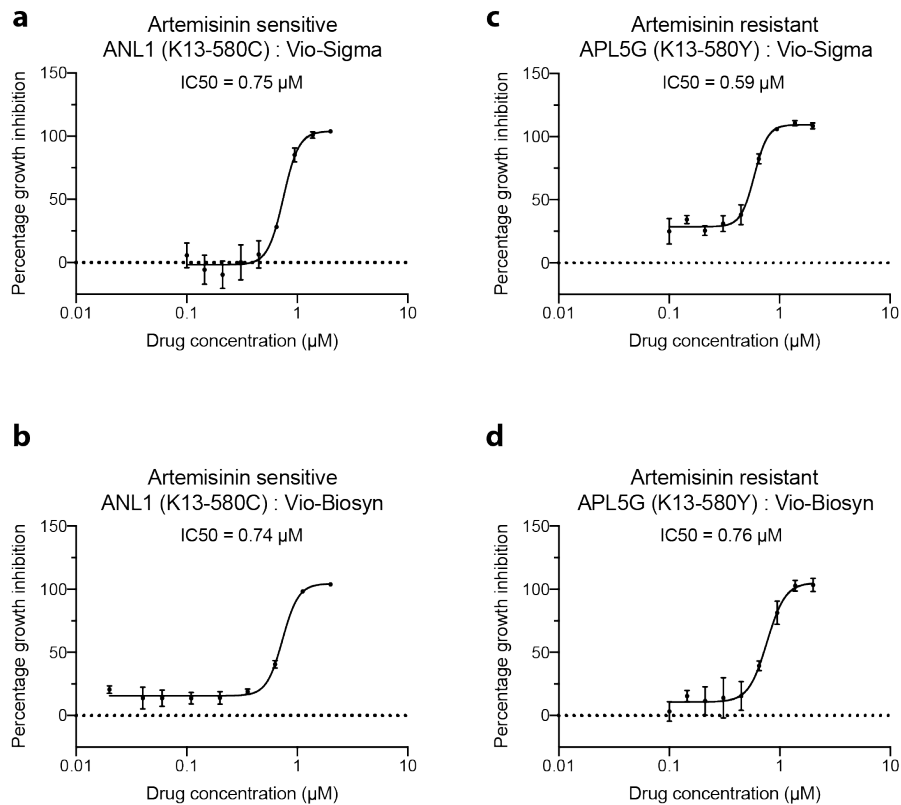
458 **a** The chemical structure of violacein (PubChem CID 11053)

459 **b-c** Commercially available violacein (b) and biosynthetic violacein (c) kill asexual 3D7

460 parasites with a half maximum inhibitory concentration of 0.51 μM (Vio-Sigma) and 0.50 μM

461 (Vio-Biosyn).

462

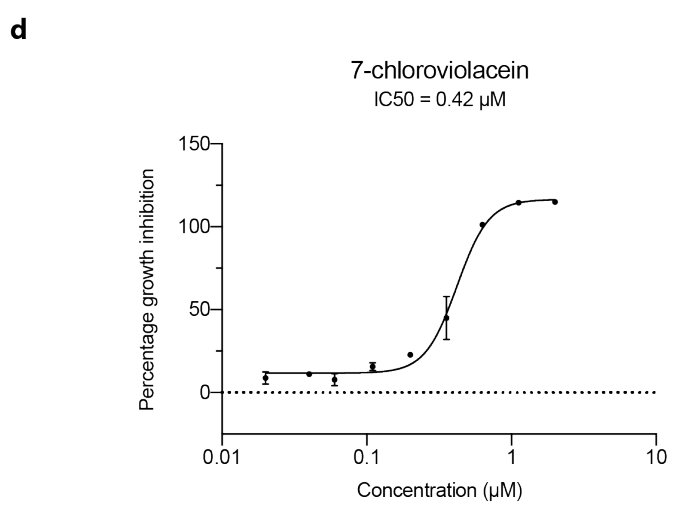
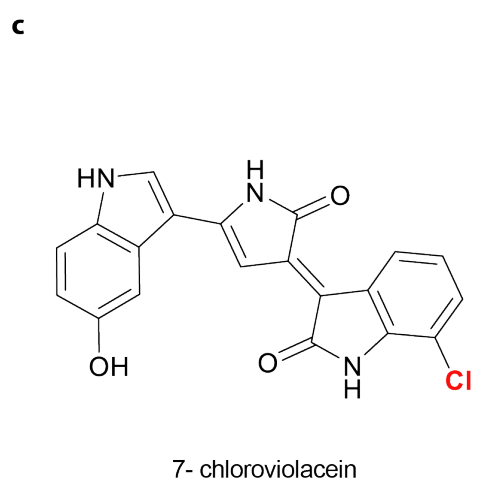
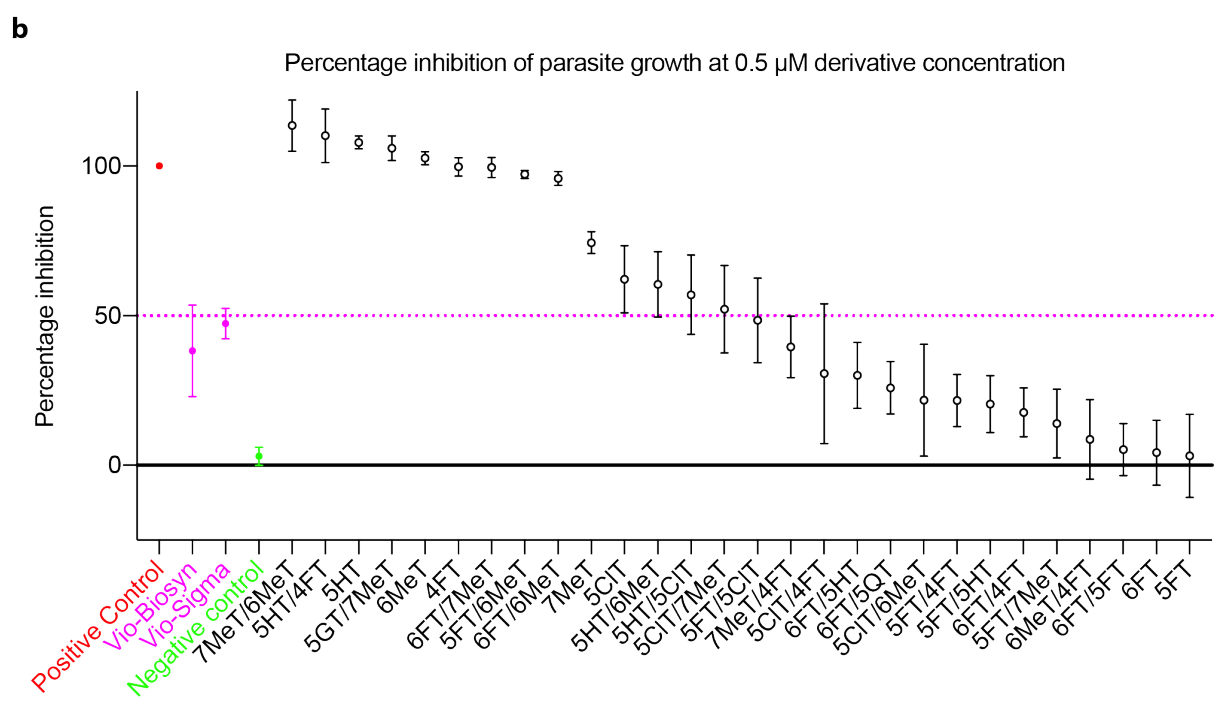
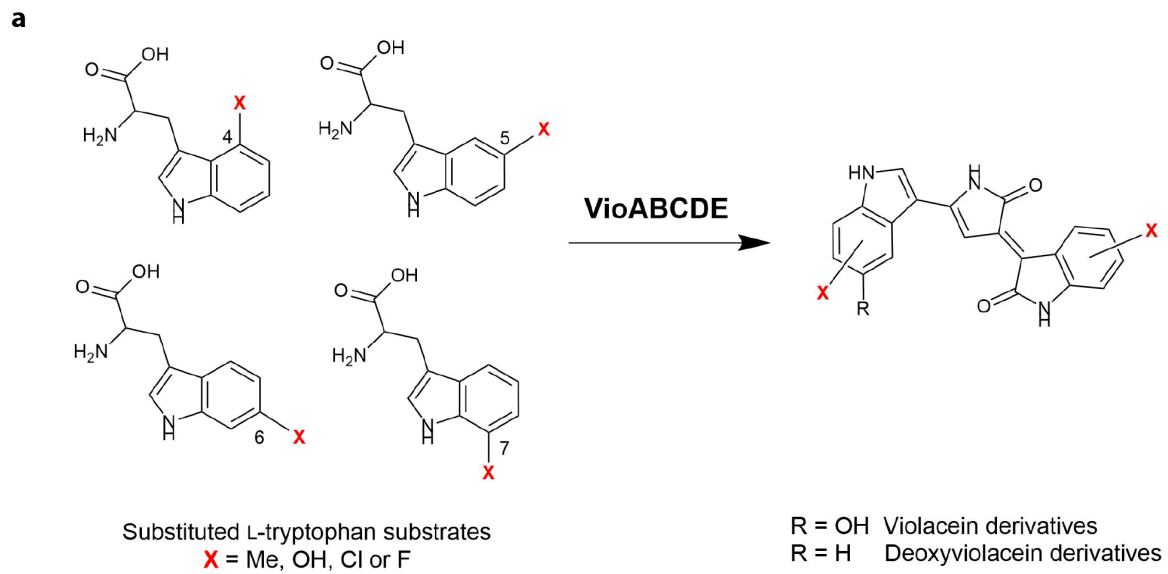


463

464 **Fig. 2:** Biosynthetic violacein kills both artemisinin-sensitive and -resistant parasite clinical
465 isolates.

466 **a-d** Both commercially available violacein and biosynthetic violacein are able to kill parasite
467 clinical isolates either sensitive (ANL1/Kelch13 wild-type, a,b) or resistant to artemisinin
468 (APL5G/Kelch13 C580Y, c,d).

469



471 **Fig. 3:** *Plasmodium falciparum* growth inhibition assays testing a series of biosynthetic
472 violacein derivatives.

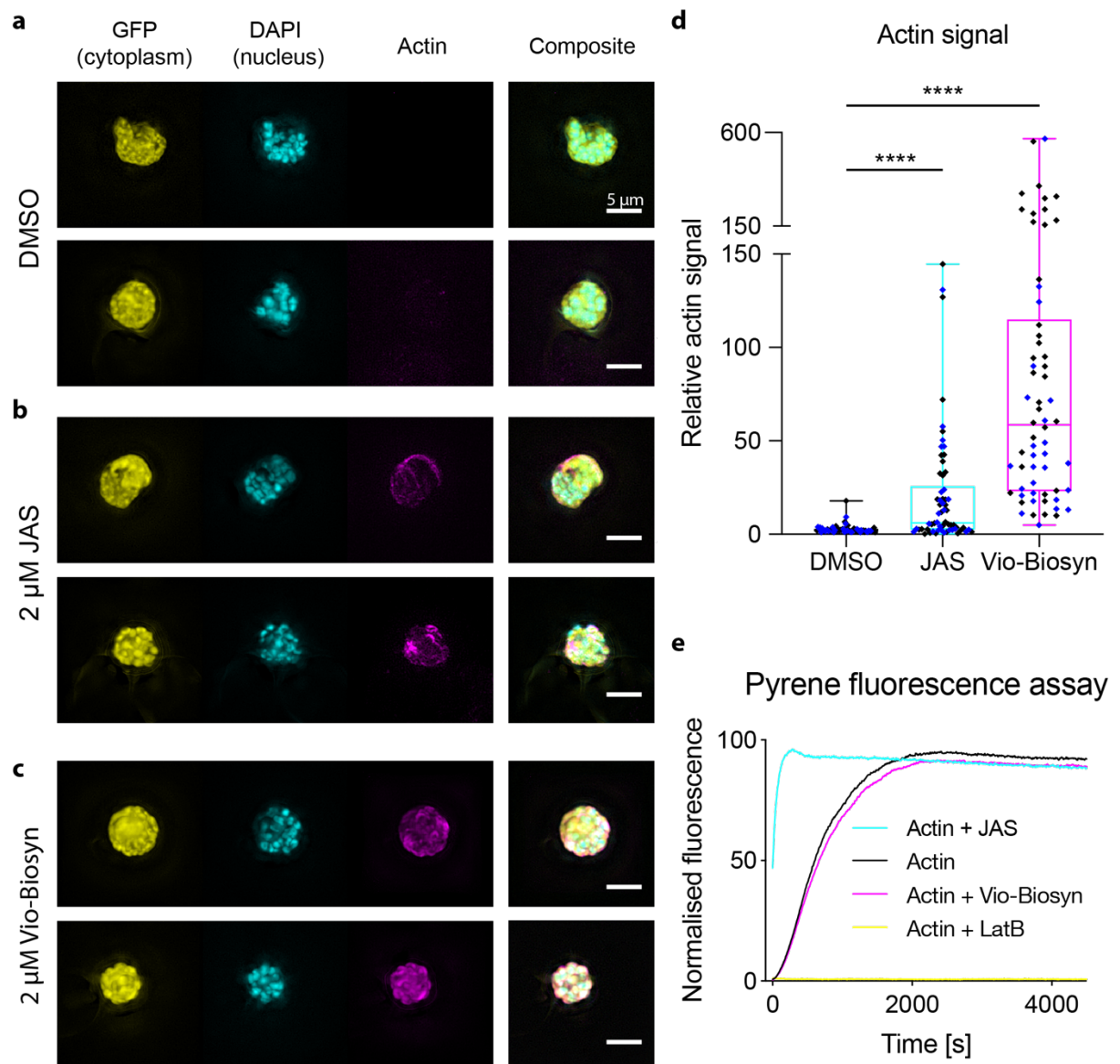
473 **a** Tryptophan derivatives (left) used to generate violacein derivatives (right).

474 **b** A screen of violacein derivative mixtures at 0.50 μM (adjusted by measuring absorbance at
475 575 nm) shows 8 mixtures >95% inhibition of parasite growth whilst 12 mixtures are less
476 potent than Vio-Biosyn.

477 **c** The chemical structure of the purified derivative 7-chloroviolaicin.

478 **d** The activity of purified violacein derivative, 7-chloroviolaicin, shows an IC_{50} value of 0.42
479 μM against 3D7 wild type parasites.

480



481

482

483 **Fig. 4:** The phenotype of biosynthetic violacein treatment on cytoplasmic GFP expressing 3D7

484 parasites suggests modulation of the actin cytoskeleton through indirect action.

485 **a** 3D7 parasites expressing cytoplasmic GFP, treated with DMSO have a diffuse actin signal.

486 **b** Parasites treated with 2 μM Jasplakinolide (JAS), which stabilises filament formation, have

487 clearly formed actin filament structures that localise to the parasite cell periphery.

488 **c** Parasites treated with 2 μM biosynthetic violacein have increased local actin concentrations

489 both around the outside of the cell and in the centre.

490 **d** Parasites treated with biosynthetic violacein have a much greater overall actin signal than
491 both DMSO control and JAS treated cells, as measured by actin fluorescence relative to
492 cytoplasmic GFP signal. Data shown is of 62 images over two biological repeats (black and
493 blue) for each sample. P values are unpaired students t-test, **** : $p < 0.0001$.

494 **e** Biosynthetic violacein shows no effect on actin polymerisation *in vitro* as measured by
495 pyrene-actin polymerization, compared to two known actin binders (Latrunculin B, which
496 binds to the monomer and prevents filament formation, and Jasplakinolide, which increases
497 nucleation and stabilises actin filaments). LatB, Latrunculin B; JAS, Jasplakinolide. Scale bar =
498 5 μm .